

SPATIAL ANALYSIS OF ANTHRACNOSE IN AVOCADO (*Persea americana* Mill.) IN DONATO GUERRA, MEXICO

Atenas **Tapia-Rodríguez**¹, José Francisco **Ramírez-Dávila**², Alfredo **Ruiz-Orta**¹,
Dulce Karen **Figueroa-Figueroa**², Agustín David **Acosta-Guadarrama**¹

¹Universidad Autónoma del Estado de México, Campus Universitario “El Cerrillo”. Facultad de Ciencias Agrícolas, Programa de Maestría y Doctorado en Ciencias Agropecuarias y Recursos Naturales. Carretera Toluca-Ixtlahuaca km 15, El Cerrillo, Piedras Blancas, Toluca, State of Mexico, Mexico. C. P. 50200.

²Universidad Autónoma del Estado de México, Campus Universitario “El Cerrillo”. Facultad de Ciencias Agrícolas, Laboratorio de Entomología y Tecnologías Aplicadas a la Agricultura de Precisión. Carretera Toluca-Ixtlahuaca km 15, El Cerrillo, Piedras Blancas, Toluca, State of Mexico, Mexico. C. P. 50200.

* Author for correspondence: jframirez@uaemex.mx

ABSTRACT

Anthracnose is a fungal disease caused by *Colletotrichum* spp. that affects the avocado (*Persea americana* Mill.) crop and causes significant economic losses in the farming sector. To focus control measures, it is important to understand the spatial distribution and the dynamics followed by the disease under field conditions. The use of methods derived from spatial statistics facilitates this task. The aim of this study was to determine the spatial behavior of anthracnose in *Persea americana* Mill. cv. Hass in Donato Guerra, a municipality in the State of Mexico, Mexico, using a geostatistical and spatial analysis by distance indices. Four hundred trees were selected and georeferenced in the municipal area. In order to measure the incidence, 48 fruits were selected from every tree. Using these data, the experimental semivariogram was estimated, and adjustments were made to models that explain the spatial arrangement. Maps were created using ordinary kriging, and the infection area was estimated. The maps generated show the presence of aggregation centers and a spatial distribution mostly fitting Gaussian and exponential models, with ranges fluctuating between 12 and 56 m, indicating spatial association between data. Likewise, the greatest percentage of infected areas was 98 %, while the lowest was 45 %. Geostatistics enables a precise understanding of the distribution patterns of diseases such as anthracnose in avocado-growing areas of the State of Mexico, which facilitates the implementation of integrated management programs with greater effectiveness.

Keywords: *Colletotrichum* spp., aggregation, geostatistics, ordinary kriging, semivariogram.

INTRODUCTION

Mexico ranks first among the 60 commercial avocado (*Persea americana* Mill.) producers in the world, with a contribution of 34.4 % of the total production volume (SIAP, 2022). This economically and nutritionally important crop is affected by phytopathogenic

Citation: Tapia-Rodríguez A, Ramírez-Dávila JF, Ruiz-Orta A, Figueroa-Figueroa DK, Acosta-Guadarrama AD. 2024. Análisis espacial de la antracnosis del aguacate (*Persea americana* Mill.) en Donato Guerra, México. *Agrociencia*. <https://doi.org/10.47163/agrociencia.v58i5.2936>

Editor in Chief:
Dr. Fernando C. Gómez Merino

Received: June 15, 2022.
Approved: March 03, 2024.
Published in Agrociencia:
July 16, 2024.

This work is licensed under a Creative Commons Attribution-Non-Commercial 4.0 International license.



agents that limit their commercialization in the international market, forcing farmers to increase their production costs and investments in chemical inputs, causing considerable environmental damage (Lemus *et al.*, 2017).

Donato Guerra is an avocado-producing municipal area in the State of Mexico, with a planted surface of 1531 ha (Figueroa-Figueroa *et al.*, 2020), contributing 13.47 % of the volume produced in the state. One of the phytosanitary problems that harms the crop is anthracnose. It is caused by species of the genus *Colletotrichum* (sexual stage *Glomerella*; Ascomycota, Sordariomycetes, Glomerellaceae), which generate round brown spots and rot the fruit pulp (Ruiz-Campos *et al.*, 2022). This situation generates economic losses for the avocado sector of the state, limiting its commercialization to the domestic market.

The implementation of methodologies such as geostatistics and spatial analysis by distance indices (SADIE) represents a viable alternative towards accurate and timely decision-making regarding crop management since they enable the analysis and interpretation of the spatial relationship of a particular phenomenon. Unlike other statistical methods that characterize the spatial model based on distributions or dispersion indices, geostatistics and SADIE consider the two-dimensional nature of disease distribution through their precise spatial location. Additionally, geostatistics, with the use of a semivariogram and ordinary kriging, enables the representation of the distribution of diseases in the form of maps, whose main function is to show spatial dispersion patterns of diseases in agricultural crops (Ramírez-Dávila *et al.*, 2002; Rivera-Martínez *et al.*, 2022).

There are currently few studies that use methodologies derived from spatial statistics to explain the behavior of fungal diseases in agricultural crops, particularly avocado. The lack of information and management alternatives leads to the incorrect implementation of strategies for the control of the disease in the crop (Cárdenas-Pardo *et al.*, 2017). The aim of this investigation was to understand the spatial distribution of anthracnose in the avocado crop in the municipal area of Donato Guerra with the use of geostatistical analysis and SADIE, assuming that the disease is found in aggregation centers in the area of study.

MATERIALS AND METHODS

Area of study

This study was carried out between January and December of 2020 in the municipal area of Donato Guerra, located in the center of the State of Mexico (19° 18' 29.87" N, 100° 8' 31.19" W) (INEGI, 2022), with an average altitude of 2200 m, a mean annual temperature of 19.2 °C, and an average rainfall of 1000 mm. The area of study is one of the main avocado-producing areas in the region (Lara-Díaz *et al.*, 2019).

Sampling method

Four hundred avocado trees were selected, georeferenced, and marked, considering one tree as a sampling unit and covering the entire surface of the municipal area with the quadrant method. The trees were verified to be 10 years old, and agronomic management was carried out in a similar manner. Every sampled tree was georeferenced using a DGPS (PRO-XR Trimble; CO, USA) to establish its geographic coordinates. Likewise, moisture, rainfall, and temperature data were taken from the Donato Guerra weather station (CONAGUA, 2022).

Each tree was classified into three strata: high, medium, and low, and four branches were chosen from each stratum, one for each cardinal point. To determine the incidence of anthracnose, 48 fruits with symptoms were selected from each branch, and samples were collected for a simultaneous study to identify and confirm the presence of *Colletotrichum gloeosporioides*. Sampling was performed biweekly between January and December 2020.

Spatial Analysis by Distance Indices (SADIE)

Using this analysis, the indices were determined based on distances for regularity (I_a) and clustering (J_a). Indices were estimated with the data gathered from a predesigned grid composed of sampling units that are assumed to be an individual counting system. A sample is said to be aggregated if $I_a > 1$, spatially random if $I_a = 1$, and regular if $I_a < 1$. A total of 2000 randomizations are sufficient to derive the values of the corresponding indices. The term C denotes the distance for clustering, that is, the minimum total distance value that sample individuals must move to gather in a unit. This value is nearer to the distance for regularity (D), using a simple direct search on all the sampling units. The sampling unit with the minimum value is referred to as the "cluster center" of the clustering. Random permutations of the observed counts result in a ratio known as Q_a (clustering probability), with a clustering distance equal to or smaller than the observed value C .

As in the case of index I_a , J_a values > 1 usually indicate an aggregated sample, $J_a = 1$ represents spatially random data, and $J_a < 1$ represents regular samples. In this way, the values of index J_a are useful to corroborate the results obtained using index I_a . Furthermore, this index is used to distinguish between spatial patterns with only one important cluster whose values are significantly greater than the unit and those with two or more clusters whose values are not significantly different from or even lower than the unit. The unit's probability (Q_a) is used to determine its significance. Because the values of I_a and J_a for random counts are uncorrelated, 2000 randomizations can be used in the software that calculates their respective values. In this work, the values and probabilities of both indices were determined using AEID 1.22. (Perry and Klukowsky, 1997).

Geostatistical analysis

Using the anthracnose incidence data collected in the area of study, a statistical estimation was performed to determine its normality. Subsequently, to obtain the

experimental semivariogram, the Variowin 2.2 program (Spring Verlag; NY, USA) was used. The experimental semivariograms were fitted to the theoretical semivariograms, obtaining the structural parameters of the model to be validated: effect, plateau, and range effects. These indicators were adjusted in a trial-and-error procedure until suitable cross-validation statistics were obtained: mean squared error, mean estimation error, and dimensionless mean squared error.

Level of spatial dependence

The level of spatial dependence was determined by dividing the nugget effect by the plateau. The result of this operation is expressed as a percentage, using the following criteria as an explanation: a result below 25 % indicates a high level of spatial dependence; values between 26 and 75 % are reported as moderate; and finally, a value above 76 % indicates a low level of spatial dependence for the data of the phenomenon under study (Lara-Díaz *et al.*, 2020; Rivera-Martínez *et al.*, 2022; Satish *et al.*, 2023).

Infected surface maps

To represent the surface infected with anthracnose, the ordinary kriging method was used, enabling the estimation of values related to points that were not sampled, thus reducing the sampling error and ensuring that the scale used was correct (Samper-Calvete and Carrera, 1996). With these estimations, maps were generated for every sampling day using the Surfer 16 program (Surface Mapping System, Golden Software Inc.; CO, USA).

RESULTS AND DISCUSSION

Spatial Analysis by Distance Indices

For the I_a index, the value was clearly located between 1.4 and 1.78. In all cases, the I_a index was significantly higher than 1 (Table 1), which indicates an aggregate spatial distribution of anthracnose inside the sampling zone. In terms of the J_a index, the lowest value was 1.11 and the highest was 1.26. In all cases, for sampling dates, the J_a index was higher than 1, but not significant in any case. However, this emphasizes the aggregation detected by the I_a index. Additionally, the J_a index indicates the number of aggregation centers present in each sample; since these values were not significantly different from the unit, the result was that anthracnose is distributed in the sampling area in more than one aggregation center. This type of distribution has been found in works such as the one by Perry and Klukowsky (1997) on aphid eggs, or Winder *et al.* (1999) on the populations of *Sitobion avenae* eggs, and Tapia-Rodríguez *et al.* (2021) on the avocado crop.

The J_a index results were not significantly higher than the unit, indicating that anthracnose is distributed across multiple aggregation foci. This coincides with Korie *et al.* (1998), who worked with beetles on winter oats in the United Kingdom,

Table 1. Value of the indices of regularity (Ia) and clustering (Ja) and their respective probabilities (Pa and Qa) on the incidence of anthracnose in *Persea americana* Mill. in the municipal area of Donato Guerra, State of Mexico, Mexico.

Month	Sampling	Ia	Pa	Ja	Qa
January	1	1.41	0.011 s	1.15	0.246 ns
	2	1.65	0.014 s	1.11	0.230 ns
February	1	1.47	0.008 s	1.20	0.282 ns
	2	1.44	0.010 s	1.22	0.269 ns
March	1	1.78	0.012 s	1.17	0.301 ns
	2	1.61	0.009 s	1.26	0.325 ns
April	1	1.57	0.014 s	1.16	0.328 ns
	2	1.50	0.009 s	1.19	0.255 ns
May	1	1.68	0.008 s	1.24	0.239 ns
	2	1.63	0.016 s	1.25	0.279 ns
June	1	1.56	0.012 s	1.22	0.244 ns
	2	1.71	0.015 s	1.21	0.299 ns
July	1	1.43	0.013 s	1.13	0.275 ns
	2	1.52	0.010 s	1.24	0.307 ns
August	1	1.66	0.012 s	1.20	0.315 ns
	2	1.74	0.013 s	1.16	0.266 ns
September	1	1.70	0.007 s	1.27	0.263 ns
	2	1.40	0.012 s	1.17	0.320 ns
October	1	1.76	0.011s	1.19	0.262 ns
	2	1.55	0.008 s	1.12	0.322 ns
November	1	1.64	0.015 s	1.13	0.251 ns
	2	1.48	0.015 s	1.18	0.286 ns
December	1	1.59	0.013 s	1.23	0.311 ns
	2	1.72	0.011 s	1.14	0.290 ns

ns: not significant; s: significant.

and Ramírez-Dávila *et al.* (2014), who studied the spatial distribution of *Sporisorium reilianum* in maize. Rivera-Martínez *et al.* (2020) performed a study on the spatial behavior of *Bactericera cockerelli* nymphs on husk tomato, in which the Ja values established the number of aggregation centers. In that study, the Ja value was not significantly greater than 1, which helped establish that the spatial distribution of the disease was concentrated in different aggregation centers.

Geostatistical analysis

Twenty-four semivariograms were estimated for the incidence of anthracnosis in avocado fruits; six of them were fitted to spherical models, nine to Gaussian models, and nine to exponential models. This helped to properly characterize spatial continuity, thus coinciding with reports by Lara-Díaz *et al.* (2020) and Cárdenas-Pardo *et al.* (2017),

who used semivariograms to analyze disease incidence in cocoa genotypes and found them to be an accurate tool for detecting spatial continuity.

The models of the semivariogram were submitted to the cross-validation process, in which the values reflected optimum ranges to continue with the geostatistical process (Isaaks and Srivastava, 1989; Harding and Deutsch, 2021). The cross-validation process has been applied in several studies in the State of Mexico to verify the accuracy of the model to which the distribution has been fitted (Lara-Díaz *et al.*, 2018; Tapia-Rodríguez *et al.*, 2020).

The nugget effect was equal to zero on all the sampling dates; therefore, the sampling error was minimal and the scale used was adequate (Table 2). The entire variation in the distribution of anthracnose is due to the spatial structure established in the corresponding semivariograms for each sampling performed, coinciding with the studies by Lara-Díaz *et al.* (2020) and dos Santos *et al.* (2023). For all sampling dates, a high level of spatial dependence was found, indicating a high spatial relationship between every sampling point.

Table 2. Parameters of the theoretical models adjusted to the anthracnose semivariograms, by sampling date, in Donato Guerra, State of Mexico, Mexico.

Sampling	Sample mean	Sample variance	Model	Nugget	Range	Plateau	Nugget/plateau (%)	Spatial dependence
January 1	6.05	12.46	Spherical	0	20.8	10.01	0	High
January 2	2.22	2.92	Gaussian	0	26.6	3.75	0	High
February 1	2.025	1.66	Gaussian	0	22.4	1.37	0	High
February 2	1.94	1.46	Spherical	0	22.4	1.44	0	High
March 1	1.47	1.25	Gaussian	0	17.6	1.14	0	High
March 2	2.92	1.64	Exponential	0	22.4	1.42	0	High
April 1	13.65	31.78	Spherical	0	28.16	16.79	0	High
April 2	3.47	2.41	Gaussian	0	20.3	2.28	0	High
May 1	3.91	2.78	Exponential	0	21.8	2.52	0	High
May 2	4.27	6.59	Gaussian	0	19.6	4.42	0	High
June 1	4.23	3.97	Gaussian	0	24.6	2.31	0	High
June 2	4.97	5.15	Exponential	0	22.8	3.64	0	High
July 1	6.55	8.14	Exponential	0	26.2	6.63	0	High
July 2	7.65	7.18	Gaussian	0	22.2	4.63	0	High
August 1	9.04	5.08	Gaussian	0	16.6	5.26	0	High
August 2	6.05	12.46	Spherical	0	21.8	10.6	0	High
September 1	5.57	9.94	Exponential	0	20.8	8.1	0	High
September 2	5.94	11.96	Exponential	0	21.9	9.12	0	High
October 1	5.86	12.36	Exponential	0	28	12.30	0	High
October 2	5.89	11.55	Gaussian	0	17.6	10.8	0	High
November 1	5.51	11.98	Spherical	0	20.8	9.56	0	High
November 2	6.02	11.39	Exponential	0	22.3	8.86	0	High
December 1	6.49	10.97	Exponential	0	19.2	10.27	0	High
December 2	5.85	13.51	Spherical	0	22.4	11.6	0	High

The spatial association range remained between 17.6 and 28.16 m, indicating the distance at which the data are spatially related. The range values found indicate that the validity of the fitted models extends to nearby distances in explaining the anthracnose aggregation phenomenon. The plateau values ranged between 1.37 and 12.3, indicating the type of aggregation present.

The maximum number of diseased fruits discovered between samplings was 12 per tree, primarily in April, June, July, and August. This is due to the presence of constant and abundant rainfall in the production area, while the decrease in temperature had an influence in January, February, October, November, and December.

Infected surface maps

The infected surface was calculated for the 24 sampling dates. The infected surface in the area of study was greater than 40 %. In both samplings, this value reached 98 %, as opposed to 45 % as the lowest value. Likewise, 24 incidence maps were created (Figure 1), which correspond to the 24 samplings conducted from January to December 2020 on a biweekly basis. These maps show aggregation centers graphically and help interpret the behavior of the disease within the study area. In all infection maps obtained, at least one aggregation center was observed, with an average of three well-defined aggregation centers, which remained present throughout the twelve months of sampling and can be seen in the upper, central, and lower right parts of each map (Figure 1).

The infection foci found in each map matched the location of avocado trees that displayed symptoms of the disease. The ordinary kriging interpolation technique has been used previously in studies related to diseases, such as those conducted by Cárdenas-Pardo *et al.* (2017) in cacao, Quiñones-Valdez *et al.* (2015) in gladiolus, and Rivera-Martínez *et al.* (2022) for the analysis of pests in avocado crops in the State of Mexico, verifying the effectiveness of kriging.

This spatial arrangement of aggregation centers indicates that the disease behaved in a stable manner, advancing from the top and bottom, with another focus in the center of the map, similar to findings by Alves *et al.* (2006) and Huded *et al.* (2022). In these studies, diseases such as anthracnose display an initial focus and then generate secondary foci, allowing the spread of the disease throughout the sampled area. Quiñones-Valdez *et al.* (2015) and Ruiz-Orta *et al.* (2023) suggest that control measures must be directed towards specific sites where the disease shows high infection rates.

It is evident that the application of geostatistical techniques helped establish the distribution and intensity of the harmful agents based on all the available spatial information used to create the maps and obtain unbiased estimates of unsampled points. These maps are highly useful since they help establish more effective control tactics. On the other hand, the characteristics related to the productive systems, such as crop age and the number of fruits selected per tree, explain the appearance of anthracnose, since older trees have been observed to be more susceptible to the disease in comparison to younger trees.

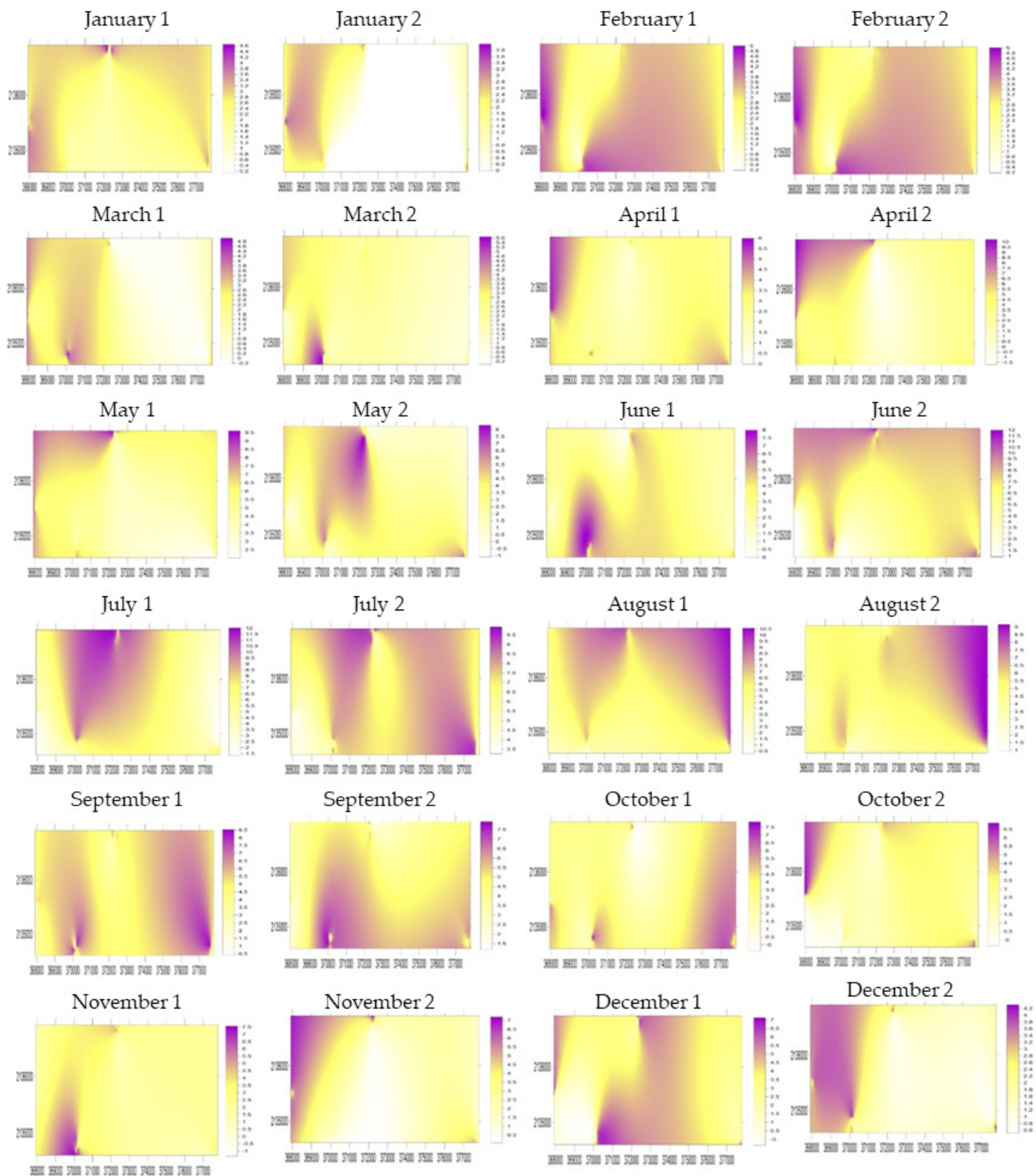


Figure 1. Biweekly maps * of the surface infected by anthracnose in *Persea americana* Mill. between January and December 2020 in Donato Guerra, State of Mexico, Mexico. *1: first fortnight of the month; 2: second fortnight of the month.

Agroclimatic conditions, such as relative humidity and rainfall in Donato Guerra, may have had a significant influence on the dynamics of the dispersal of the disease, particularly between April and September, where the presence of infection foci can be observed. Another important factor in the dissemination and possible progress of anthracnose were the management practices that the farmers used on the trees. The use of contaminated tools to prune and harvest fruits favors the transportation of the inoculum to healthy plants. During the samplings, few farmers were observed to remove the branches and leaves from pruning, which is why *C. gloeosporioides* remained in the orchards.

CONCLUSIONS

Anthracnose in the municipal area of Donato Guerra displayed an aggregate spatial distribution, forming infection foci that remained stable during the entire sampling period. The aggregate spatial distribution of the disease in *Persea americana* Mill. obtained with the use of spatial analysis by distance indices was verified with geostatistical analysis and the maps created using kriging. The creation of maps of the infested surface helped detect areas with a high percentage of infection, which will help propose alternatives directed at a timely, efficient, and sustainable phytosanitary management of the avocado crop in Donato Guerra.

ACKNOWLEDGEMENTS

To the National Science and Technology Council for the scholarship granted for postgraduate studies. To the avocado farmers in the municipal area of Donato Guerra.

REFERENCES

- Alves MC, Pozza EA, Machado JC, Araújo DV, Talamini V, Oliveira MS. 2006. Geoestatística como metodologia para estudar a dinâmica espaço-temporal de doenças associadas a *Colletotrichum* spp. transmitidos por sementes. *Fitopatologia Brasileira* 31 (1): 557–563. <https://doi.org/10.1590/s0100-41582006000600004>
- Cárdenas-Pardo NJ, Darghan A, Sosa-Rico MD, Rodríguez A. 2017. Análisis espacial de la incidencia de enfermedades en diferentes genotipos de cacao (*Theobroma cacao* L.) en El Yopal (Casanare), Colombia. *Acta Biológica Colombiana* 22 (2): 209–220.
- CONAGUA (Comisión Nacional del Agua). 2022. Red de estaciones climatológicas. Gobierno de México. Secretaría del Medio Ambiente y Recursos Naturales. Comisión Nacional del Agua. Servicio Meteorológico Nacional. Ciudad de México, México. <https://smn.conagua.gob.mx/es/climatologia/informacion-climatologica/informacion-estadistica-climatologica> (Retrieved: March 2024).
- dos Santos MP, de Mates EC, Santos Neto B de M, Cardoso ACP, Leite SA, Moreira AA, Albuquerque EVS, Fernandes DRR, Hilliou F, de Carvalho GA, Castellani MA. 2023. Morphometric variation and fluctuating asymmetry in populations of *Closterocerus coffeellae*

- (Ihering) (Hymenoptera: Eulophidae) in different management and landscape of coffee agroecosystems. <https://doi.org/10.2139/ssrn.4665544>
- Figueroa-Figueroa DK, Ramírez-Dávila JF, Antonio-Némiga X, González-Huerta A. 2020. Cartografía del aguacate en el sur del Estado de México mediante tratamiento digital de imágenes sentinel-2. *Revista Mexicana de Ciencias Agrícolas* 11 (4): 865–879. <https://doi.org/10.29312/remexca.v11i4.2173>
- Harding B, Deutsch CV. 2021. Trend modeling and modeling with a trend. In Deutsch JL. (ed.), *Geostatistics Lessons. Resource Modeling Solutions*: Calgary, Canada. 14 p.
- Huded S, Pramesh D, Chittaragi A, Sridhara S, Chidanandappa E, Prasannakumar MK, Shamshiri RR. 2022. Spatial distribution patterns for identifying risk areas associated with false smut disease of rice in Southern India. *Agronomy* 12 (12): 2947. <https://doi.org/10.3390/agronomy12122947>
- INEGI (Instituto Nacional de Estadística, Geografía e Informática). 2022. Anuario de estadísticas por entidad federativa. Ciudad de México, México. <https://www.inegi.org.mx/app/biblioteca/ficha.html?upc=889463901846> (Retrieved: March 2024).
- Isaaks EH, Srivastava RM. 1989. An introduction to applied geostatistics. Oxford University Press: New York, NY, USA, pp: 35–38.
- Korie S, Clark SJ, Perry JN, Muggleston MA, Bartlett PW, Marshall EJP, Mann JA. 1998. Rejoinder analyzing maps of dispersal around a single focus. *Environmental and Ecological Statistics* 5 (4): 349–351. <https://doi.org/10.1023/a:1009603804998>
- Lara-Díaz AV, Ramírez-Dávila JF, Maldonado-Zamora FI, Figueroa-Figueroa DK, Acosta-Guadarrama AD, Rivera-Martínez R, Némiga XA. 2018. Simulación espacial de *Claviceps gigantea* (Fuentes, de la Isla, Ullstrup y Rodríguez) en el Estado de México. *Revista Mexicana de Ciencias Agrícolas* 9 (1): 95–109. <https://doi.org/10.29312/remexca.v9i1.850>
- Lara-Díaz AV, Ramírez-Dávila JF, Maldonado-Zamora FI, Rivera-Martínez R, Acosta-Guadarrama AD, Lara-Vázquez F. 2020. Modelización espacial de las poblaciones de *Oligonychus perseae* (Tuttle, Baker y Abatiello, 1976) en el Estado de México. *Revista Fitotecnia Mexicana* 43 (4): 411–419.
- Lara-Díaz AV, Ramírez-Dávila JF, Rubí-Arriaga M, Campos-Alanis J, Maldonado-Zamora FI, Rivera-Martínez R, Acosta-Guadarrama AD. 2019. Modelización espacial de *Oligonychus perseae* (Tuttle, Baker y Abatiello) mediante técnicas geoestadísticas. *Revista Mexicana de Ciencias Agrícolas* 10 (6): 1405–1416. <https://doi.org/10.29312/remexca.v10i6.1951>
- Lemus C, Bugarín J, Grageola F, Rodríguez JG, Mejía K, Valdivia R. 2017. Características químicas de la pasta de aguacate Hass fruto completo (*Persea americana* Mill.) mexicano de Nayarit destinado a la alimentación animal. *Revista Computadorizada de Producción Porcina* 24 (2): 212–218.
- Perry N, Klukowsky Z. 1997. Spatial distributions of counts at the edges of sample areas. In VI Conference of the Biometric Society. International Biometric Society: Cordoba, Spain, pp: 103–108.
- Quiñones-Valdez R, Sánchez-Pale JR, Pedraza-Esquivel AK, Castañeda-Vildozola A, Gutierrez-Ibañez AT, Ramírez-Dávila JF. 2015. Análisis espacial de *Thrips* spp. (Thysanoptera) en el cultivo de gladiolo en la región sureste del Estado de México, México. *Southwestern Entomologist* 40 (2): 397–408. <https://doi.org/10.3958/059.040.0213>
- Ramírez-Dávila J, González-Andújar JL, Ocete R, Martínez LM. 2002. Descripción geoestadística de la distribución espacial de los huevos del mosquito verde *Jacobiasca lybica* (Bergenin

- & Zanon) (Homoptera: Cicadellidae) en viñedo: modelización y mapeo. *Boletín Sanidad Vegetal de Plagas* 28 (1): 87–95.
- Ramírez-Dávila JF, Sánchez-Pale JR, Figueroa-Figueroa DK, de León C. 2014. Asociación espacial de largo plazo de *Sporisorium reilianum* en el cultivo de maíz. *Revista Mexicana de Micología* 40 (1): 37–45.
- Rivera-Martínez R, Ramírez-Dávila JF, Martínez-Quiroz M, González-Huerta A. 2020. Modelización espacial de ninfas de *Bactericera cockerelli* Sulc. en tomate de cáscara (*Physalis ixocarpa* Brot.) por medio de técnicas geoestadísticas. *Biotecnia* 22 (1): 142–152. <https://doi.org/10.18633/biotecnia.v22i1.1162>
- Rivera-Martínez R, Ramírez-Dávila JF, Tapia-Rodríguez A, Figueroa-Figueroa DK, Acosta-Guadarrama AD, Serrato-Cuevas R. 2022. Comportamiento espacial del barrenador de la rama en aguacate utilizando el método del SADIE en el Estado de México. *Revista Mexicana de Ciencias Agrícolas* 13 (2): 247–259. <https://doi.org/10.29312/remexca.v13i2.2728>
- Ruiz-Campos C, Umaña-Rojas G, Gómez-Alpizar L. 2022. Identificación multilocus de especies de *Colletotrichum* asociadas a la antracnosis de papaya. *Agronomía Mesoamericana* 33 (1): 45495. <https://doi.org/10.15517/am.v33i1.45495>
- Ruiz-Orta A, Tapia-Rodríguez A, Figueroa-Figueroa DK, Ramírez-Dávila JF. 2023. Analysis of the spatial association of fumagina (*Capnodium* spp.) and green scale (*Coccus viridis*) in coffee in Sultepec, Mexico. *Agrociencia* 57 (7). <https://doi.org/10.47163/agrociencia.v57i7.2945>
- Samper-Calvete FJ, Carrera J. 1996. *Geoestadística: aplicaciones a la hidrología subterránea* (Segunda edición). Centro Internacional de Métodos en Ingeniería: Barcelona, España. 484 p.
- Satish Y, Shekhar S, Rathod ASS, Chouksey N. 2023. Spatial variability of soil micronutrients in Raichur district of Karnataka. *International Journal of Statistics and Applied Mathematics* 8 (4): 560–567.
- SIAP (Servicio de Información Agroalimentaria y Pesquera). 2022. Sistema de información agroalimentaria de consulta nueva generación (SIACON). Gobierno de México. Sistema de información agroalimentaria de consulta nueva generación (SIACON NG). Ciudad de México, México. <https://www.gob.mx/siap/documentos/siacon-ng-161430> (Retrieved: March 2024).
- Tapia-Rodríguez A, Ramírez-Dávila JF, Aquino-Martínez JG, Arriaga MR, Ruiz-Orta A. 2021. Determination of the spatial behavior of anthracnose in avocado cultivation using spatial statistics. *Investigación Agraria* 23 (2): 63–72. <https://doi.org/10.18004/investig.agrar.2021.diciembre.2302697>
- Tapia-Rodríguez A, Ramírez-Dávila JF, Figueroa-Figueroa DK, Salgado-Siclán ML, Serrato-Cuevas R. 2020. Análisis espacial de antracnosis en el cultivo de aguacate en el Estado de México. *Revista Mexicana de Fitopatología* 38 (1): 132–145. <https://doi.org/10.18781/r.mex.fit.1911-1>
- Winder L, Perry JN, Holland JM. 1999. The spatial and temporal distribution of the grain aphid *Sitobion avenae* in winter wheat. *Entomologia Experimentalis et Applicata* 93 (3): 275–288. <https://doi.org/10.1046/j.1570-7458.1999.00588.x>